

Microwave-assisted hydrothermal synthesis of N-doped titanate nanotubes for visible-light-responsive photocatalysis

Yen-Ping Peng^a, Shang-Lien Lo^{a,*}, Hsin-Hung Ou^{a,b}, Shiau-Wu Lai^c

^a Research Center for Environmental Pollution Prevention and Control Technology, Graduate Institute of Environmental Engineering, National Taiwan University, 71 Chou-Shan Rd., Taipei 106, Taiwan

^b W.M. Keck Laboratory, California Institute of Technology, Pasadena, CA 91125, USA

^c Department of Chemical Engineering and Materials Science, Yuan-Ze University, Taiwan

ARTICLE INFO

Article history:

Received 31 May 2010

Received in revised form 20 July 2010

Accepted 20 July 2010

Available online 30 July 2010

Keywords:

Titanate nanotubes

Nitrogen doped

Visible-light

Photocatalysis

ABSTRACT

This study employs a rapid, energy frugal and environmental friendly method to synthesize nitrogen doped titanate nanotubes (NTNTs), and uses TEM, XRD, Raman, nitrogen adsorption–desorption isotherms analysis, and UV–vis spectroscopy to characterize the obtained NTNTs. TEM results demonstrate that the current research successfully synthesized one-dimensional NTNTs via the microwave hydrothermal (M-H) method, and show that NTNTs retain a tubular structure after sintering at a temperature of 350 °C. XRD results agree well with Raman spectrum findings. Both show that the intensity of anatase crystallization increases with an increase in sintering temperature. After sintering at high temperature, above 250 °C, the UV–vis absorbance edges of NTNTs significantly shift to the visible-light region, which illustrates N atom doping into nanotubes. Photocatalytic tests conclude that the NTNTs-350 shows good efficiency with visible-light response.

© 2010 Elsevier B.V. All rights reserved.

1. Introduction

Research has intensively investigated titanate nanotubes (TNTs) due to one-dimensional nanostructure, large internal and external surfaces, ion exchangeability, and photocatalytic activity. These advantages lead to various applications such as solar cells, photocatalysis, and electroluminescent devices [1–5]. However, the TNTs high band gap between 3.3 eV and 3.87 eV obstructs application [6]. In other words, only UV light, which occupies less than 5% of the solar spectrum, excites TNTs. Therefore, studies have made great attempts to extend the absorption of TNTs to visible-light-sensitization. Particle size [7,8], manipulation of oxygen vacancy [9,10], and doping are the major ways to engineer the TiO₂ band gap. Some of the methods have used various transition metals [11–13] and anions such as F, S, C, and N [14–17] as dopants for increasing the photocatalytic efficiency of TiO₂ under visible-light. Only a few studies have focused on TNTs band gap reduction [18–23]. In 2004, Tokudome and Miyauchi [23] first examined the visible-light activity of N-doped TNTs. Geng et al. [24] proposed that instead of substituting O₂[−] ions in the TNTs lattice, the doping N is likely located at the interstitial sites. Jiang et al. [18], Wu et al. [20], and Qamar et al. [19] successfully synthesized N-doped

TNTs, C-doped TNTs, and Ni-TNTs, to reduce TNTs band gap and shift absorbance to the visible-light region.

Since the first discovery of TNTs [25,26], many methods have attempted to synthesize TNTs including the sol–gel process [27], electrochemical anodic oxidation [28–30], and hydrothermal treatment [5,31–34]. Among these methods, hydrothermal treatment has attracted much attention owing to cost-effectiveness and convenience to synthesize TNTs with excellent morphology. However, the typical hydrothermal procedure, synthesized at 110–130 °C in autoclave for 20–120 h, is relatively time- and energy-consuming. A previous study used a novel method, modified from the traditional hydrothermal method, with microwave assistance, namely microwave hydrothermal treatment (M-H treatment), to synthesize TNTs [2]. M-H treatment has several advantages such as shorter reaction time, lower energy usage, and enhancing the wall-structure intensity of TNTs. Previous study successfully synthesized TNTs under 400W irradiation at 130 °C for only 1.5 h with S_{BET} values of 256 m² g^{−1} and found the TNTs preferentially assigned for Na_xH_{2−x}Ti₃O₇, with a vague rutile phase and no clear anatase phase. Unfortunately, similar to the traditional hydrothermal method, the TNTs prepared by the M-H method showed weak photocatalytic activity.

This study dopes nitrogen into TNTs via M-H treatment for the first time to seek an expeditious, energy saving way to synthesize nitrogen doped titanate nanotubes (NTNTs), excited under visible-light.

* Corresponding author. Tel.: +886 2 23625373; fax: +886 2 23928830.
E-mail address: sll@ntu.edu.tw (S.-L. Lo).

2. Experiment

2.1. Preparation of N-doped titanate nanotubes

The experiment used a microwave digestion system (Ethos Touch Control, MILESTONE Corporation), with a double-walled vessel consisting of an inner Teflon liner and outer shell of high strength Ultem polyetherimide. In a typical procedure, described in the literatures [2,17], 0.6 g of TiO₂ (Degussa P25) was added into 70 mL of 10 M NaOH in a Teflon container. The M-H reaction was promulgated at 450 W, 130 °C for 3 h, and cooled to room temperature. The applied temperature, irradiation power, and time of treatment were programmable by computer. After the M-H process, the white powders were washed by mixing three times with 0.5N HCl, followed by washing five times with de-ionized water. Afterward, the white powders were dried at -57.8 °C and 100–200 mTorr for 12 h to obtain TNTs. Nitrogen doped titanate nanotubes (NTNTs) were prepared following the experimental report by Jiang et al. [18] and modified with M-H treatment to shorten synthesized time, conserve energy, and enhance anatase crystal structure. The as-prepared TNTs were dispersed in a 70 mL solution with a 1:1 volume ratio of ethanol and water containing 20 wt% NH₄Cl. After stirring for 30 min, the mixing solution was heated by the M-H process at 450 W, 130 °C for 2 h. The white powders were then filtrated and washed with de-ionized water and ethanol, alternatively, and dried at the same conditions of previous works of TNTs. To convert the nanotube layers into anatase, the samples were sintered fewer than 20% O₂/80% N₂ at different temperatures of 250 °C, 350 °C, and 450 °C for 2 h.

2.2. Characterization

Microstructure and morphology of the synthesized materials were observed on a HR-TEM (JEOL-JEM2100) at an accelerate voltage of 200 kV. The Brunauer–Emmett–Teller (BET, Micromeritics, model ASAP 2020) specific area (S_{BET}) was determined by a multi-point BET method using the adsorption data in the relative pressure range from 0.05 to 0.30. The crystal structures of TNTs and NTNTs-X (X refers to the sintered temperature) were characterized by

X-ray diffraction (Rigaku-TTRAX III) with Cu K α radiation and a Raman spectrometer (Dimension-P2). UV–vis spectroscopy (GBC-cintra 202), which used BaSO₄ as the reflectance standard, was applied to investigate the absorbance spectra of NTNTs-X over a range of 200–900 nm.

2.3. Photocatalytic activity tests

Photocatalytic performance of the as-synthesized NTNTs-X was investigated by degradation of MO (methyl orange) solution under 15 W commercial fluorescent lamps. A 500 mL solution of MO of concentration 10 ppm was added into the vessel and the required amount of the catalyst (1 g L⁻¹) was added to the solution. Before irradiation, the solution was magnetically stirred for 60 min in a dark chamber to allow adsorption equilibration. The MO degradation was monitored by measuring the change in absorbance on a UV–vis spectrophotometer (GBC-cintra 20). The absorbance of MO was followed at a wavelength of 508 nm. For each experiment, the rate constant was calculated from the initial slope obtained by linear regression.

3. Results and discussion

3.1. Structure and morphology

Fig. 1 shows the TEM images of TNTs, NTNTs-350, NTNTs-450, and the HR-TEM image of NTNTs-350. The image in Fig. 1(a) reveals that the as-prepared TNTs have a tubular structure with a crystalline multiwall, and the lengths measure several hundred nanometers. Fig. 1(b) demonstrates that the NTNTs retain a tubular structure after sintering at 350 °C. However, sintering at 450 °C may destroy the tubular structure and convert it to rod morphology, as Fig. 1(c) shows. Hafez [35] showed the similar result of titanate nanotubes transferring to titanate nanorods after sintering at 450 °C for 30 min. Yu et al. [36] reported that the nanotubes calcined at 400 °C are fibrous in nature and have a large surface area and high pore volume. The thermal stability of TNTs has been confirmed to be dependent on the Na amount within the TNT structure [37,38]. BET results, summarized in Table 1, demonstrate the slight

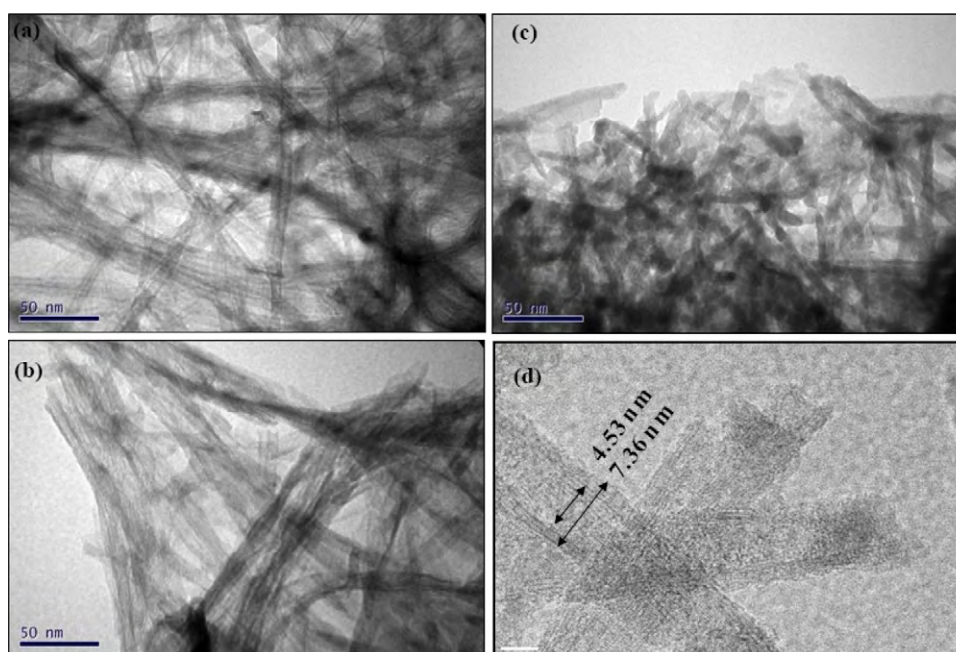


Fig. 1. TEM images of (a) TNTs, (b) NTNTs-350, (c) NTNTs-450, (d) HR-TEM image of NTNTs-350.

Table 1

S_{BET} , absorbent wavelength and photon energy of TNTs, NTNTs-250, NTNTs-350, and NTNTs-450.

	S_{BET} (m^2g^{-1})	Absorbent wavelength (nm)	Photon energy (eV)
TNTs	367.0	380	2.85
NTNTs-250	283.4	410	2.57
NTNTs-250 (mild)	283.4	545	1.68
NTNTs-350	216.8	412	2.55
NTNTs-350 (mild)	216.8	570	1.51
NTNTs-450	149.6	405	2.69

damages of the TNTs structure after calcinations with a surface area of $367.0\text{ m}^2\text{ g}^{-1}$, $283.4\text{ m}^2\text{ g}^{-1}$, $216.8\text{ m}^2\text{ g}^{-1}$ and $149.6\text{ m}^2\text{ g}^{-1}$ for TNTs, NTNTs-250, NTNTs-350 and NTNTs-450, respectively. The HR-TEM image (Fig. 1(d)) clearly shows that the NTNTs-350 retains a tubular structure after sintering at 350°C and indicates that the inner and outer diameters of the nanotubes are 4.53 nm and 7.36 nm, respectively.

This study used X-ray diffraction to perform structural characterizations of the as-prepared titanate nanotubes and nitrogen doped titanate nanotubes, sintered at different temperatures. Fig. 2(a) and (b) shows the XRD patterns for TNTs and NTNTs. Both figures show peaks appearing at the diffraction angles of 9.58° , 24.01° , 28.68° , and 48.23° , related to the nanotube structure [1,2,32,39]. The diffraction angle of 28.68° also indicates abouting Na atoms intercalating within the TNTs structure. A similar feature in XRD patterns of TNTs have been shown in previous research [37,1,40]. Our previous study synthesized TNTs via M-H treatment with different irradiation powers and found TNTs preferentially assigned for $\text{Na}_x\text{H}_{2-x}\text{Ti}_3\text{O}_7$, with a vague rutile phase and no clear anatase phase [2]. This corresponds to the anatase phase as the preferred phase in synthesizing TNTs [41,42]. The XRD patterns of NTNTs-250, NTNTs-350, and NTNTs-450 show the characteristic peaks at $2\theta = 25^\circ$, 38° , 48° , 54° , 55° and 63° corresponding to the anatase phase. Fig. 2 reveals the change in crystal structure from nanotubes (JCPDS 41-192) to anatase (JCPDS 37-0951) after calcinations. Notably, the change from Fig. 2(c) to (e) shows an interesting phenomenon, that the anatase peak intensity increases with increasing calcination temperature, indicating improved crystallization. Further, combining the TEM images and the XRD patterns, gives the preliminary result that NTNTs-350 shows anatase crystalline and retains the tubular structure. In other words, NTNTs-350 is a novel material with good photo-degradation ability and high surface area, advantageous for environmental engineering applications.

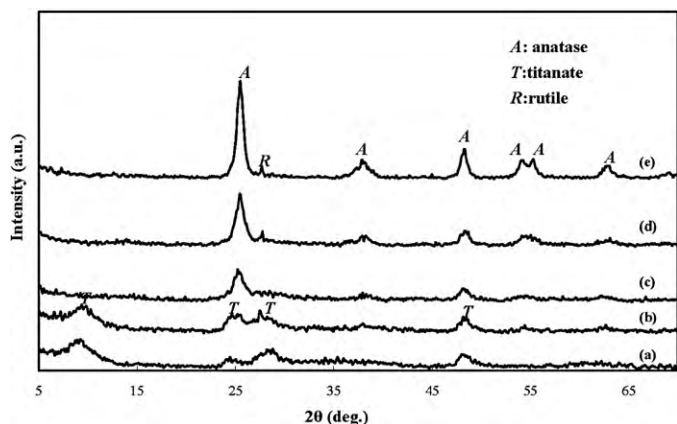


Fig. 2. XRD patterns of (a) TNTs, (b) NTNTs, (c) NTNTs-250, (d) NTNTs-350, (e) NTNTs-450.

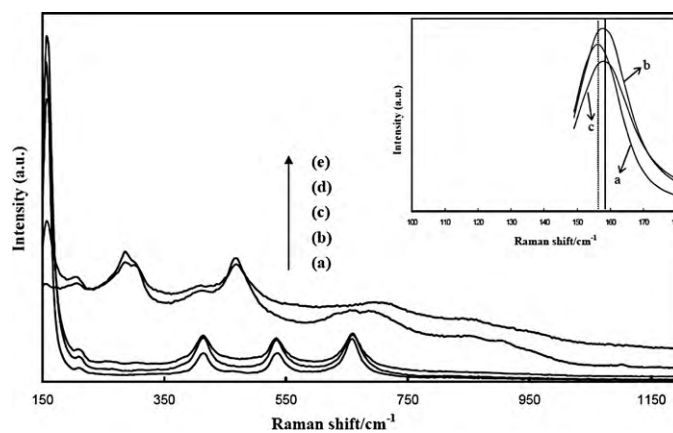


Fig. 3. Raman spectra of (a) TiO_2 , (b) NTNTs-450, (c) NTNTs-350, (d) NTNTs, and (e) TNTs. Inset plot shows the enlarged Raman spectrum around 160 cm^{-1} .

Raman spectroscopy results confirmed the XRD findings. The spectrum of the TiO_2 particle in Fig. 3(a) shows lattice vibrations at 414 cm^{-1} , 534 cm^{-1} , and 661 cm^{-1} , characteristic for anatase [43,44]. Fig. 3(b) and (c) shows similar peak positions represented for NTNTs-450 and NTNTs-350. Inspection of the Raman spectrum for TiO_2 , NTNTs-350, and NTNTs-450 at around 156 cm^{-1} (the inset plot in Fig. 3), shows a slight shift that illustrates that nitrogen doped into the TNTs structure changes the crystalline. Fig. 3(d) and (e) both show the bands at 292 cm^{-1} and 474 cm^{-1} , assigned to the nanotube structure [45,46]. Accordingly, the bands at 450 cm^{-1} and 668 cm^{-1} could be assigned to Ti–O–Ti vibrations, where 917 cm^{-1} was attributed to Ti–O–Na vibrations in the interlayer regions of the nanotube walls [46]. In Raman spectra of nanotubes, the vibrating band at 665 cm^{-1} shifts to 691 cm^{-1} and 705 cm^{-1} for NTNTs and TNTs. The peak at 917 cm^{-1} is not clearly detectable that could be explained by the low Na^+ ions in nanotubes due to the acid washing procedure. The Raman spectrum outcomes consisting of XRD analyses, show successfully synthesized N-doped titanate nanotubes by the microwave-assisted hydrothermal process, and an enhanced anatase phase of NTNTs after annealing at high temperature.

3.2. Optical properties

This study used UV–vis spectroscopy to investigate the absorption spectra of TNTs, NTNTs-250, NTNTs-350, and NTNTs-450. The spectrum of TNTs and NTNTs-450 shows single sharp edges with the band gap absorption onset at 375 nm and 402 nm. Meanwhile, the calcined N-doped nanotubes exhibit a high tailing absorbance in the longer wavelength, giving two absorption edges. The mild absorbance was estimated at about 540 nm and 574 nm in the visible-light region for NTNTs-350 and NTNTs-250. Similar second adsorption phenomena are also described in Bellardita et al. [47] and Shao et al. [48]. To determine the catalyst band gaps, Fig. 4 inset establishes the Tauc Plot [49]. Extra polation of these lines to the photon energy axis yields the band gaps shown in Table 1. Nitrogen doped TNTs show a strong adsorption versus TNTs throughout the visible region, ascribed to the light yellow color appearance. This apparel observation clearly illustrates that the presence of N results in the formation of additional energy levels above the TNT valence band [50–52].

3.3. Photocatalytic activities

Fig. 5 displays the time-dependence degradation of MO over NTNTs prepared at different temperatures. No significant MO photodegradation occurred in the absence of catalysts under 15 W

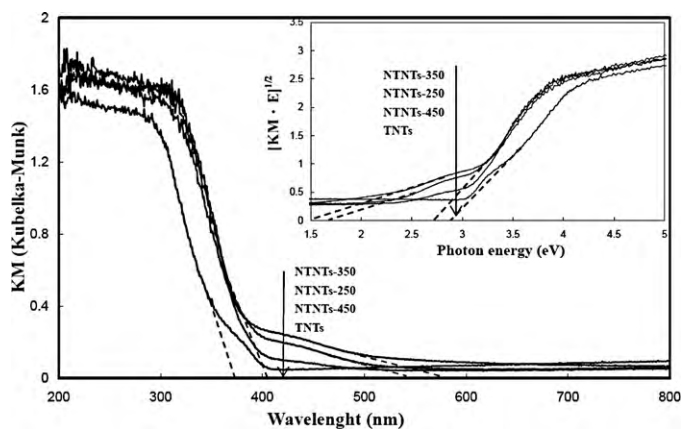


Fig. 4. UV-vis absorbance of TNTs and NTNTs-250, NTNTs-350, and NTNTs-450. Inset plot shows the square root of the Kubelka–Munk function versus the photon energy.

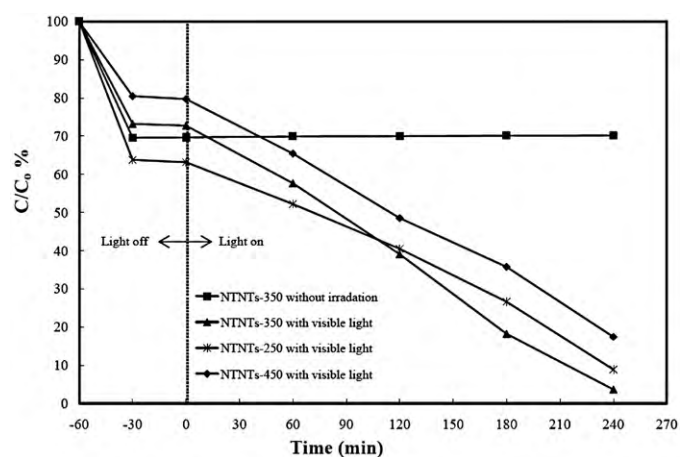


Fig. 5. Photo-degradation of methyl orange over NTNTs-X with and without visible-light irradiation.

commercial fluorescent lamps irradiation for 4 h. Without the presence of illumination, MO commenced to degrade right after adding catalysts into the MO and then achieved adsorption equilibrium at 60 min. This result appears to be attributed to the photo induced adsorption of MO molecules. An interesting finding is that the higher the S_{BET} of catalysts, the more MO was adsorbed (see Table 1). After 240 min illumination, the MO degradation efficiencies reached 91.2%, 82.6% and 96.3% MO for NTNTs-250, NTNTs-350 and NTNTs-450, respectively. Also, the pseudo first-order rate constants of MO degradation were obtained at 0.224 min^{-1} , 0.257 min^{-1} and 0.296 min^{-1} . The TNTs does not possess photocatalytic activity and are not suitable photocatalysts for degrading organic compounds because they consist of the titanate phase rather than phases of TiO_2 [19]. In this study, we reported that anatase phase TNTs can be illuminated under visible-light by doping N atoms into TNTs. To sum up, this study ascribes the high activity of NTNTs to better crystallization, relatively high S_{BET} and intensive visible-light absorption, as evidenced by HR-TEM, XRD, Raman, and UV-vis DRS results.

4. Conclusions

This study successfully synthesizes nitrogen doped titanate nanotubes through the microwave hydrothermal method in only 3 h. This procedure is a time saving, energy frugal, and environmental friendly method compared to the traditional hydrothermal

method. TEM, nitrogen adsorption–desorption isotherms analysis, XRD, Raman, and UV-vis DRS investigated these materials in detail. The results reveal that N-doped titanate nanotubes consist of a tubular structure with a high anatase phase after annealing at 350°C . With an increase in sintering temperature, the intensity of anatase crystallization increases, but the surface area of NTNTs-X decreases. The band gap of NTNTs-350 reduces to 1.51 eV by doping nitrogen into titanate nanotubes, and the prepared samples show high photo-degradation ability of methyl orange under visible-light illumination.

Acknowledgement

This work was financially supported by the National Science Council, Taiwan (NSC 98-2211-E-002-040-MY3).

References

- [1] X. Sun, Y. Li, Synthesis and characterization of ion-exchangeable titanate nanotubes, *Chem. Eur. J.* 9 (2003) 2229–2238.
- [2] H.H. Ou, S.L. Lo, Y.H. Liou, Microwave-induced titanate nanotubes and the corresponding behaviour after thermal treatment, *Nanotechnology* 18 (2007) 175702–175707.
- [3] M. Hodos, E. Horvath, H. Haspel, A. Kukovec, Z. Konya, I. Kiricsi, Photosensitization of ion-exchangeable titanate nanotubes by CdS nanoparticles, *Chem. Phys. Lett.* 399 (2004) 512–515.
- [4] A. Kukovec, M. Hodos, Z. Konya, I. Kiricsi, Complex-assisted one-step synthesis of ion-exchangeable titanate nanotubes decorated with CdS nanoparticles, *Chem. Phys. Lett.* 411 (2005) 445–449.
- [5] C.C. Tsai, J.N. Nian, H.H. Teng, Mesoporous nanotube aggregates obtained from hydrothermally treating TiO_2 with NaOH, *Appl. Surf. Sci.* 253 (2006) 1898–1902.
- [6] J.S. Jang, W. Li, S.H. Oh, J.S. Lee, Fabrication of CdS/ TiO_2 nano-bulk composite photocatalysts for hydrogen production from aqueous H_2S solution under visible light, *Chem. Phys. Lett.* 425 (2006) 278–282.
- [7] J.C. Tristao, F. Magalhaes, P. Corio, M.T.C. Sansiviero, Electronic characterization and photocatalytic properties of CdS/ TiO_2 semiconductor composite, *J. Photochem. Photobiol., A* 181 (2006) 152–157.
- [8] A. Kongkanand, K. Tvrđy, K. Takechi, M. Kuno, P.V. Kamat, Quantum dot solar cells: tuning photoresponse through size and shape control of CdSe- TiO_2 architecture, *J. Am. Chem. Soc.* 130 (2008) 4007–4015.
- [9] H. Ma, G.H. Ma, W.J. Wang, X.X. Gao, H.L. Ma, Size-dependent optical properties and carriers dynamics in CdSe/ZnS quantum dots, *Chinese Phys. B* 17 (2008) 1280–1285.
- [10] Y. Bai, Y. Cao, J. Zhang, M. Wang, R. Li, P. Wang, S.M. Zakeeruddin, M. Graetzel, High-performance dye-sensitized solar cells based on solvent-free electrolytes produced from eutectic melts, *Nat. Mater.* 7 (2008) 626–630.
- [11] T.E. Agustina, H.M. Ang, V.K. Vareek, A review of synergistic effect of photocatalysis and ozonation on wastewater treatment, *J. Photochem. Photobiol., C* 6 (2005) 264–273.
- [12] H. Lin, C.P. Huang, W. Li, C. Ni, S.I. Shah, Y.H. Tseng, Size dependency of nanocrystalline TiO_2 on its optical property and photocatalytic reactivity exemplified by 2-chlorophenol, *Appl. Catal., B* 68 (2006) 1–11.
- [13] J.O. Carneiro, V. Teixeira, A. Portinha, A. Magalhaes, P. Coutinho, C.J. Tavares, R. Newton, Iron-doped photocatalytic TiO_2 sputtered coatings on plastics for self-cleaning applications, *Mater. Sci. Eng. B* 138 (2007) 144–150.
- [14] D. Crisan, N. Dragan, M. Crisan, M. Raeanu, A. Braileanu, M. Anastasescu, A. Lanculescu, D. Mardare, D. Luca, V. Marinescu, A. Moldovan, Crystallization study of sol-gel un-doped and Pd-doped TiO_2 materials, *J. Phys. Chem. Solids* 69 (2008) 2548–2554.
- [15] E.B. Gracien, J. Shen, X. Sun, D. Liu, M. Li, S. Yao, J. Sun, Photocatalytic activity of manganese, chromium and cobalt-doped anatase titanium dioxide nanoporous electrodes produced by reanodization method, *Thin Solid Films* 515 (2007) 5287–5297.
- [16] H. Imahori, S. Hayashi, T. Uemeyama, S. Eu, A. Oguro, S. Kang, Y. Matano, T. Shishido, S. Ngamsinlapasathian, S. Yoshikawa, Comparison of electrode structures and photovoltaic properties of porphyrin-sensitized solar cells with TiO_2 and Nb, Ge, Zr-added TiO_2 composite electrodes, *Langmuir* 22 (2006) 11405–11411.
- [17] H.H. Ou, C.H. Liao, Y.H. Liou, J.H. Hong, S.L. Lo, Photocatalytic oxidation of aqueous ammonia over microwave-induced titanate nanotubes, *Environ. Sci. Technol.* 42 (2008) 4507–4512.
- [18] Z. Jiang, F. Yang, N. Luo, B.T.T. Chu, D. Sun, H. Shi, T. Xiao, P.P. Edwards, Solvothermal synthesis of N-doped TiO_2 nanotubes for visible-light-responsive photocatalysis, *Chem. Commun.* (2008) 6372–6374.
- [19] M. Qamar, S.J. Kim, A.K. Ganguli, TiO_2 -based nanotubes modified with nickel: synthesis, properties, and improved photocatalytic activity, *Nanotechnology* 20 (2009) 455703–455710.

- [20] Z. Wu, F. Dong, W. Zhao, H. Wang, Y. Liu, B. Guan, The fabrication and characterization of novel carbon doped TiO₂ nanotubes, nanowires and nanorods with high visible light photocatalytic activity, *Nanotechnology* 20 (2009) 235701–235709.
- [21] Y. Wang, C. Feng, Z. Jin, J. Zhang, J. Yang, S. Zhang, A novel N-doped TiO₂ with high visible light photocatalytic activity, *J. Mol. Catal. A: Chem.* 260 (2006) 1–3.
- [22] C. Feng, Y. Wang, Z. Jin, J. Zhang, S. Zhang, Z. Wu, Z. Zhang, Photoactive centers responsible for visible-light photoactivity of N-doped TiO₂, *New J. Chem.* 32 (2008) 1038–1047.
- [23] H. Tokudome, M. Miyauchi, N-doped TiO₂ nanotube with visible light activity, *Chem. Lett.* 33 (2004) 1108–1109.
- [24] J. Geng, D. Yang, J. Zhu, D. Chen, Z. Jiang, Nitrogen-doped TiO₂ nanotubes with enhanced photocatalytic activity synthesized by a facile wet chemistry method, *Mater. Res. Bull.* 44 (2009) 146–150.
- [25] T. Kasuga, M. Hiramatsu, A. Hoson, T. Sekino, K. Niihara, Formation of titanium oxide nanotube, *Langmuir* 14 (1998) 3160–3163.
- [26] T. Kasuga, M. Hiramatsu, A. Hoson, T. Sekino, K. Niihara, Titania nanotubes prepared by chemical processing, *Adv. Mater.* 11 (1999) 1307–1311.
- [27] O.K. Varghese, M. Paulose, K. Shankar, G.K. Mor, C.A. Grimes, Water-photolysis properties of micron-length highly-ordered titania nanotube-arrays, *J. Nanosci. Nanotechnol.* 5 (2005) 1158–1165.
- [28] A. Ghicov, H. Tsuchiya, J.M. Macak, P. Schmuki, Titanium oxide nanotubes prepared in phosphate electrolytes, *Electrochem. Commun.* 7 (2005) 505–509.
- [29] H. Tsuchiya, J.M. Macak, L. Taveira, E. Balaur, A. Ghicov, K. Sirotna, P. Schmuki, Self-organized TiO₂ nanotubes prepared in ammonium fluoride containing acetic acid electrolytes, *Electrochem. Commun.* 7 (2005) 576–580.
- [30] A. Thorne, A. Kruth, D. Tunstall, J.T.S. Irvine, W. Zhou, Formation, Structure, and stability of titanate nanotubes and their proton conductivity, *J. Phys. Chem. B* 109 (2005) 5439–5444.
- [31] S. Zhang, W. Li, Z. Jin, J. Yang, J. Zhang, Z. Du, Z. Zhang, Study on ESR and inter-related properties of vacuum-dehydrated nanotubed titanic acid, *J. Solid State Chem.* 11 (2004) 1365–1371.
- [32] Q. Chen, W.Z. Zhou, G.H. Du, L.M. Peng, Trititanate nanotubes made via a single alkali treatment, *Adv. Mater.* 14 (2002) 1208–1211.
- [33] D.V. Bavykin, S.N. Gordeev, A.V. Moskalenko, A.A. Lapkin, F.C. Walsh, Apparent two-dimensional behavior of TiO₂ nanotubes revealed by light absorption and luminescence, *J. Phys. Chem. B* 109 (2005) 8565–8569.
- [34] H.H. Ou, S.L. Lo, Review of titania nanotubes synthesized via the hydrothermal treatment: fabrication, modification, and application, *Sep. Purif. Technol.* 58 (2007) 179–191.
- [35] H.S. Hafez, Synthesis of highly-active single-crystalline TiO₂ nanorods and its application in environmental photocatalysis, *Mater. Lett.* 63 (2009) 1471–1474.
- [36] J. Yu, H. Yu, B. Cheng, C. Trapalis, Effects of calcination temperature on the microstructures and photocatalytic activity of titanate nanotubes, *J. Mol. Catal. A.* 249 (2006) 135–142.
- [37] E. Morgado, M.A.S. de Abreu, O.R.C. Pravia, B.A. Marinkvic, P.M. Jardim, F.C. Rizzo, A.S. Araújo, A study on the structure and thermal stability of titanate nanotubes as a function of sodium content, *Solid State Sci.* 8 (2006) 888–900.
- [38] C.C. Tsai, H. Teng, Structural features of nanotubes synthesized from NaOH treatment on TiO₂ with different post-treatments, *Chem. Mater.* 18 (2006) 367–373.
- [39] X. Ding, X.G. Xu, Q. Chen, L.M. Peng, Preparation and characterization of Fe-incorporated titanate nanotubes, *Nanotechnology* 17 (2006) 5423–5427.
- [40] L.Q. Weng, S.H. Song, S. Hodgson, A. Baker, J. Yu, Synthesis and characterisation of nanotubular titanates and titania, *Eur. Ceram. Soc.* 26 (2006) 1405–1409.
- [41] C.C. Tsai, H. Teng, Regulation of the physical characteristics of titania nanotube aggregates synthesized from hydrothermal treatment, *Chem. Mater.* 16 (2004) 4352–4358.
- [42] E. Morgado, M.A.S. de Abreu, O.R.C. Pravia, B.A. Marinkvic, P.M. Jardim, F.C. Rizzo, A.S. Araújo, A study on the structure and thermal stability of titanate nanotubes as a function of sodium content, *Solid State Sci.* 8 (2006) 888–900.
- [43] P.H. Hsiao, K.P. Wang, C.H. Cheng, H.S. Teng, Nanocrystalline anatase TiO₂ derived from a titanate-directed route for dye-sensitized solar cells, *Photochem. Photobiol. A* 188 (2007) 19–24.
- [44] L. Qian, Z.L. Du, S.y. Yang, Z.S. Jin, Raman study of titania nanotube by soft chemical process, *J. Mol. Struct.* 749 (2005) 103–107.
- [45] J.A. Toledo-Antonio, S. Capula, M.A. Cortes-Jacome, C. Angeles-Chavez, E. Lopez-Salinas, G. Ferrat, J. Navarrete, J. Escobar, Low-temperature FTIR study of CO adsorption on titania nanotubes, *J. Phys. Chem. C* 111 (2007) 10799–10805.
- [46] M.A. Cortés-Jácome, G. Ferrat-Torres, L.F. Flores Ortiz, C. Angeles-Chávez, E. López-Salinas, J. Escobar, M.L. Mosqueira, J.A. Toledo-Antonio, In situ thermo-Raman study of titanium oxide nanotubes, *Catal. Today* 126 (2007) 248–255.
- [47] M. Bellardita, M. Addamo, A. Di Paola, L. Palmisano, A.M. Venezia, Preparation of N-doped TiO₂: characterization and photocatalytic performance under UV and visible light, *Phys. Chem. Chem. Phys.* 11 (2009) 4084–4093.
- [48] G.S. Shao, F.Y. Wang, T.Z. Ren, Y. Liu, Z.Y. Yuan, Hierarchical mesoporous phosphorus and nitrogen doped titania materials: synthesis, characterization and visible-light photocatalytic activity, *Appl. Catal., B* 92 (2009) 61–67.
- [49] J. Tauc, R. Grigorvici, A. Vancu, Optical properties and electronic structures of amorphous germanium, *Phys. Stat. Sol.* 15 (1996) 627–637.
- [50] H. Irie, Y. Watanabe, K. Hashimoto, Nitrogen-concentration dependence on photocatalytic activity of TiO_{2-x}N_x powders, *J. Phys. Chem. B* 107 (2003) 5483–5486.
- [51] S. Mozia, M. Tomaszewska, B. Kosowska, B. Grzmil, A.W. Morawski, K. Kalucki, Decomposition of nonionic surfactant on a nitrogen-doped photocatalyst under visible-light irradiation, *Appl. Catal. B: Environ.* 55 (2005) 195–200.
- [52] T. Ihara, M. Miyoshi, Y. Iriyama, O. Matsumoto, S. Sugihara, Visible-light-active titanium oxide photocatalyst realized by an oxygen-deficient structure and by nitrogen doping, *Appl. Catal. B: Environ.* 42 (2003) 403–409.